

# Metabisulfite as an Unconventional Reagent for Green Oxidation of Emerging Contaminants Using an Iron-Based Catalyst

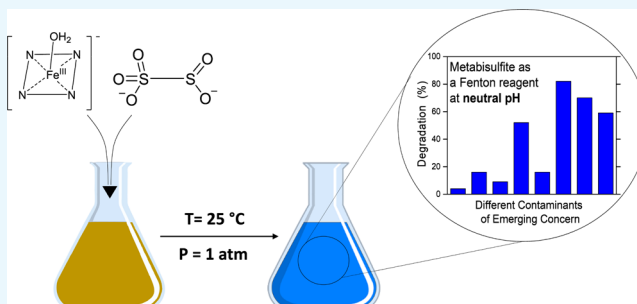
Giulio Farinelli,<sup>†</sup> Marco Minella,<sup>‡</sup> Fabrizio Sordello,<sup>‡</sup> Davide Vione,<sup>\*,‡</sup> and Alberto Tiraferri<sup>\*,†</sup>

<sup>†</sup>Department of Environment, Land and Infrastructure Engineering (DIATI), Politecnico di Torino, Corso Duca degli Abruzzi 24, 10129 Turin, Italy

<sup>‡</sup>Department of Chemistry, University of Turin, Via Pietro Giuria 5, 10125 Turin, Italy

## S Supporting Information

**ABSTRACT:** In this work, contaminants of emerging concern were catalytically degraded in the homogeneous phase with the use of unconventional green reagents. Three reagents, namely, sulfite, metabisulfite, and persulfate, were tested and compared with conventional hydrogen peroxide in the degradation process activated by Fe-TAML. The latter is a biodegradable, homogeneous tetra-amido macrocyclic ligand catalyst containing iron(III). Metabisulfite showed the highest efficiency among the three tested reagents, and its reactivity was similar to that of H<sub>2</sub>O<sub>2</sub>. However, metabisulfite is a safer and cleaner reagent compared to H<sub>2</sub>O<sub>2</sub>. A comprehensive study of the activity of metabisulfite with Fe-TAML was carried out toward the oxidative degradation of eight contaminants of emerging concern. The catalytic process was tested at different pH values (7, 9, and 11). Metabisulfite showed the highest activity at pH 11, completely degrading some of the tested micropollutants, but in several cases, the system was active at pH 9 as well. In particular, metabisulfite showed the best efficiency toward phenolic compounds. A preliminary study on the reaction mechanism and the nature of the active species in the Fe-TAML/metabisulfite system was also conducted, highlighting that a high-valent iron-oxo species might be involved in the degradation pathways.



## 1. INTRODUCTION

Micropollutants, such as pesticides, pharmaceuticals, and personal care products, are persistent and biologically active substances. They are ubiquitous in aquatic environments and can jeopardize the life of plants, animals, and humans.<sup>1</sup> The Fenton reaction is a promising advanced oxidation process to reduce micropollutants in water, and it has been proven effective for the degradation of a wide variety of recalcitrant and/or non-biodegradable contaminants in industrial wastewaters.<sup>2</sup> The main reactions involved in Fenton oxidation cause the formation of reactive species, such as—mainly—hydroxyl radicals and/or superoxidized iron species.<sup>2–4</sup> The Fenton process works best in the pH range of 2.5–4, with the highest degradation rates usually observed around pH 3.<sup>5</sup>

Living organisms metabolize micropollutants and potentially toxic endogenous and exogenous compounds with cytochrome P450, an iron-based family of enzymes.<sup>6</sup> On this basis, Collins and co-workers have developed an innovative catalyst for water decontamination, the Fe-TAML activator, which mimics the oxidative activity of cytochrome P450 by forming a stable iron-oxo species in water when it reacts with peroxides.<sup>7</sup> Fe-TAML has a large spectrum of applications in the removal of recalcitrant micropollutants and pathogens from water.<sup>8–11</sup> Its reaction usually takes place at room temperature and it is most effective in the pH range 7.5–11, with the highest rates usually observed around pH 10–11.<sup>12</sup> An oxidation process that is

efficient under basic conditions may be more promising and useful than a process operating under acidic conditions (e.g., the traditional Fenton process), for two main reasons: (i) it does not require pH adjustments when the water effluent is already alkaline, as in the case of some industrial effluents; (ii) it allows the coprecipitation of inorganic cations (e.g., toxic metals) potentially present in the effluent, thus reducing the need of an ad hoc treatment step and preventing their possible interfering activity.<sup>13,14</sup> In this sense, oxidation by Fe-TAML or other similar catalysts as tools to improve the Fenton reaction is potentially advantageous compared to a classic Fenton process.

Hydrogen peroxide is preferentially used as the Fenton reagent because of its relatively low cost, availability on the market, and fair environmental compatibility. Hydrogen peroxide is also the preferred reagent in the case of oxidations activated by Fe-TAML.<sup>7–11</sup> In addition to hydrogen peroxide, Fe-TAML can activate hypochlorite, organic peroxides, and oxone.<sup>10,15</sup> However, not all these alternative reagents are convenient in every circumstance. For instance, hypochlorite may lead to the formation of potentially carcinogenic chlorinated byproducts.<sup>16–19</sup> Organic peroxides and oxone,

**Received:** September 20, 2019

**Accepted:** November 13, 2019

**Published:** November 25, 2019

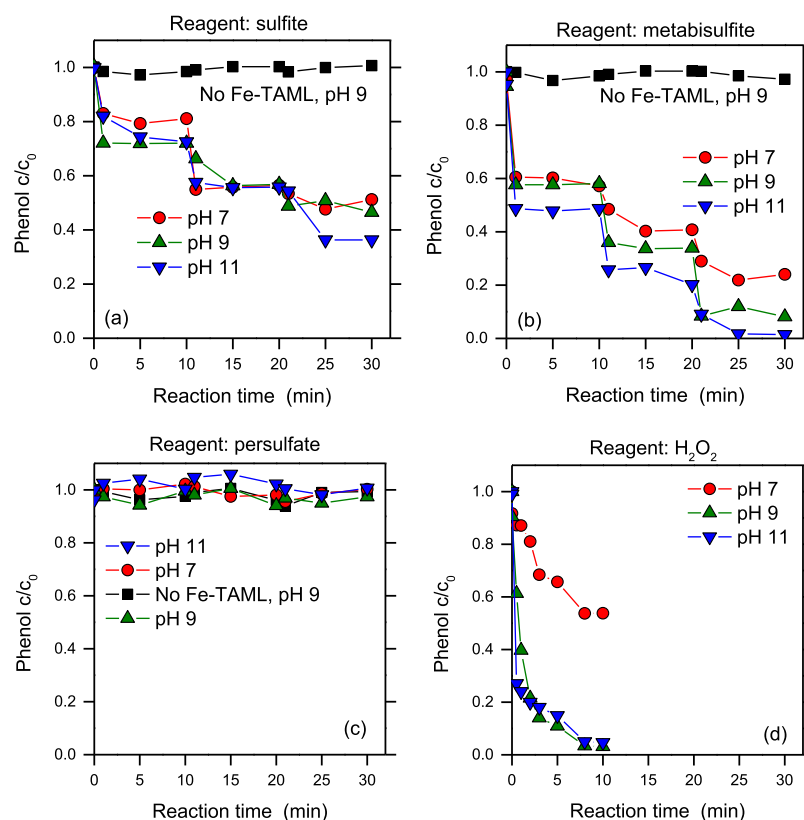


**Figure 1.** Degradation of phenol with different reagents. Reagents were (a) sulfite, (b) metabisulfite, (c) persulfate, and (d)  $\text{H}_2\text{O}_2$ . The reactions were carried out in phosphate buffer (10 mM) by adding 0.1 mM of reagent every 10 min (i.e., at  $t = 0, 10,$  and  $20$  min), with the exception of  $\text{H}_2\text{O}_2$  that was added only once at the beginning ( $t = 0$ ). Initial conditions were  $[\text{Fe-TAML}] = 0.01$  mM;  $[\text{PhOH}] = 0.1$  mM.

besides being explosive and unsafe, have a high cost. Therefore, they may not be easily employed to treat large flow rates, which are commonly encountered in wastewater treatment plants.<sup>20,21</sup> While being the current best choice, hydrogen peroxide has also important limitations related to operational safety, particularly when it is used in large amounts and concentrations.  $\text{H}_2\text{O}_2$  is highly reactive, and it forms explosive mixtures upon contact with organic compounds.<sup>22</sup> Furthermore, it is corrosive and irritant for eyes, mucous membranes and skin, and its relatively high vapor pressure poses health risks by inhalation even following short exposure.<sup>22</sup>  $\text{H}_2\text{O}_2$  has also been classified as a known animal carcinogen, with unknown relevance on humans.<sup>23</sup> Finally, the thermodynamic instability of  $\text{H}_2\text{O}_2$  results in a relatively short shelf life, especially when stored in concentrated solutions and exposed to ambient temperatures. For all these reasons, research is needed to identify more benign reagents that combine all of the positive features of hydrogen peroxide while minimizing safety hazards and operational burdens.

In preliminary tests, we found that benign species, such as sulfite and metabisulfite, can be effectively activated by Fe-TAML toward the degradation of micropollutants. Despite its activity as a reductant, sulfite can be activated toward the oxidative degradation of organic compounds.<sup>24–26</sup> On the other hand, to the best of our knowledge, no report is present in the literature regarding this peculiar reactivity of metabisulfite,  $\text{S}_2\text{O}_5^{2-}$ . It is a potentially low-cost, low-risk, and eco-friendly reagent, with limited health effects (e.g., it is used to preserve alcoholic beverages) and a demonstrated absence of carcinogenic activity.<sup>27</sup> Given its generally reducing nature, metabisulfite is sometimes used as a quencher of

oxidative processes, such as Fenton or hypochlorite treatments.<sup>28,29</sup>

This work offers a comprehensive study of the activity of metabisulfite with Fe-TAML toward the oxidative degradation of a selection of environmental micropollutants of increasing worldwide concern. A discussion on the reaction mechanism and the nature of the active species in the Fe-TAML/metabisulfite system (as it will be shown below, iron-oxo rather than radical based) is also provided. Fe-TAML is a well-known green catalyst for the oxidative degradation of various organic contaminants and other compounds.<sup>7</sup> However, the discovery of cleaner and safer reagents different from those previously proposed (e.g.,  $\text{H}_2\text{O}_2$ ) is a breakthrough in the field of advanced oxidation processes because it opens the route toward greener cleaning systems.

## 2. RESULTS AND DISCUSSION

**2.1. Performance of Different Reagents toward the Degradation of Phenol.** The activity of hydrogen peroxide in the degradation of various classes of contaminants with Fe-TAML is widely reported in the literature.<sup>9–11,30,31</sup> Therefore, here,  $\text{H}_2\text{O}_2$  was used as a comparative standard. Figure 1 shows the catalytic degradation of phenol in three-step addition experiments, using Fe-TAML and sulfite ( $\text{SO}_3^{2-}$ , Figure 1a), metabisulfite ( $\text{S}_2\text{O}_5^{2-}$ , Figure 1b), persulfate ( $\text{S}_2\text{O}_8^{2-}$ , Figure 1c), and hydrogen peroxide (Figure 1d, only one addition) as reagents. After each addition of metabisulfite (one every 10 min, i.e., at 0, 10, and 20 min reaction time), there was significant phenol degradation, soon followed by stabilization of the phenol concentration, with an overall step-like trend that closely mirrored the step-wise  $\text{S}_2\text{O}_5^{2-}$  additions. This finding is

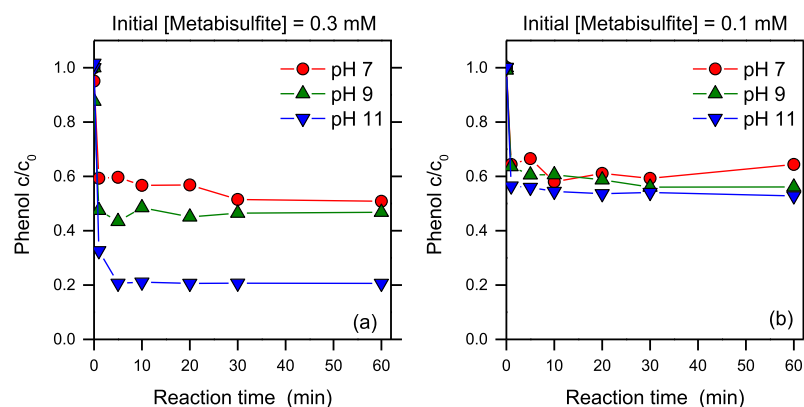


**Figure 2.** Degradation of phenol with metabisulfite as the reagent. The reactions were carried out in phosphate buffer (10 mM), with initial concentrations  $[\text{Fe-TAML}] = 0.01 \text{ mM}$ ;  $[\text{PhOH}] = 0.1 \text{ mM}$ , and adding one aliquot of metabisulfite with initial concentrations of (a) 0.3 and (b) 0.1 mM.

similar to recent results, obtained in the framework of the traditional Fenton reaction.<sup>32</sup> Duplicates and triplicates of these tests are presented in Figure S1 of the [Supporting Information](#). The replicate tests showed high robustness, implying the reproducibility of the adopted experimental procedures. All of the reactions were quenched by decreasing the pH to a final value  $<3$ . Under acidic conditions, demetallation (decomplexation of the Fe-TAML complex) is promoted and the catalytic reaction is stopped as a consequence, also considering the limited reactivity of Fe(III) species with  $\text{H}_2\text{O}_2$  and similar reagents under very acidic conditions.<sup>33</sup>

Metabisulfite was more effective than sulfite toward phenol degradation, and the highest degradation efficiency for the two reagents was achieved at pH 11. On the other hand, persulfate did not show any activity toward the degradation of phenol (further insights below). Table S1 of the [Supporting Information](#) reports the degradation percentages reached at the end of the degradation experiments for all of the investigated conditions. Wherever a significant reactivity was observed (i.e., with sulfite, metabisulfite, and mainly hydrogen peroxide), phenol degradation was very fast immediately after the addition of the reagent. It then followed a rapid stabilization of the substrate concentration. This behavior prevented the details of the degradation kinetics to be monitored with the used experimental setup, which was based on sample aliquots withdrawal from the reaction beaker, quenching of the reaction, and successive high-performance liquid chromatography (HPLC) quantification of the residual substrate concentration. As a consequence, we could not measure the initial reaction rate. However, we could easily measure the degradation percentage, which is the most relevant information in the framework of water treatment. Additionally, such an approach allowed us to obtain sufficient insight into the reaction mechanism (vide infra). The first step of the reaction might be investigated by using the rather outmoded (and, unfortunately, not easily found nowadays) stopped-flow technique, which has proven, for instance, suitable for the investigation of the dark traditional Fenton process.<sup>34</sup>

In general, the degradation efficiency was higher at basic pH values. Because phenol undergoes acid–base equilibrium ( $\text{p}K_a$  9.95),<sup>35</sup> at pH 9, the phenolate anion ( $\text{PhO}^-$ ) starts to be significantly present, while at pH 11, it prevails. Phenolate is more easily oxidized than neutral PhOH. In the case of  $\text{H}_2\text{O}_2$ ,

an almost complete degradation of phenol took place at both pH 9 and 11 with just one hydrogen peroxide addition. In contrast, at pH 7, the  $\text{H}_2\text{O}_2$  treatment was less effective. The pH trend of the degradation efficiency was consistent with that reported by Collins et al. when using  $\text{H}_2\text{O}_2$ ;<sup>12</sup> please see further details in the [Supporting Information](#).

Interestingly, the system containing Fe-TAML + persulfate was unable to induce significant degradation of phenol at any of the investigated pH values. It may be reasonable to assume that the inactivity of persulfate depends on poor complexation capability (steric hindrance) of the persulfate anion with the metal center of Fe-TAML (vide infra).<sup>36,37</sup>

The reported results suggest that metabisulfite is less effective than hydrogen peroxide in the degradation of phenol, but it is the most effective among the alternative reagents investigated here. Because of the lower cost and hazards of metabisulfite compared to  $\text{H}_2\text{O}_2$ , its reaction conditions were optimized, and its potential as a  $\text{H}_2\text{O}_2$  substitute was further investigated for the degradation of other contaminants of emerging concern (CECs). Some phenol degradation experiments were carried out to identify the experimental conditions able to maximize its transformation with metabisulfite. In particular, we wanted to assess whether the best degradation conditions could be reached with multistep additions of metabisulfite at relatively low concentration, or with a single addition of the reagent at higher concentration. Figure 2 shows the results of the experiments carried out with Fe-TAML and metabisulfite at different pH values (7, 9, and 11), with only one addition of the reagent at concentrations of 0.3 mM (Figure 2a) and 0.1 mM (Figure 2b; this latter experiment is similar to the first addition step reported in Figure 1b). Phenol concentration was monitored for up to 60 min. As expected, the reaction was very fast in the first 1–2 min after the addition of the reagent and it followed a rapid stabilization of phenol concentration afterward. The overall degradation performance was better when the concentration of metabisulfite was higher (i.e., 0.3 mM), but the best results were definitely achieved when the same overall amount of metabisulfite was added in three separate steps (100% degradation, see Figure 1b), rather than in a single addition (80% degradation, Figure 2a). It is reasonable to assume that, in the case of a single large addition, the reagent itself partly scavenges the reactive species, as often observed in the classic Fenton process (note that metabisulfite has a reducing character). In fact, within the same time interval, more reagent (higher concentration of metabisulfite)

is available to react with the reactive species present in the system, compared with the addition of the same overall amount of the reagent in separate steps.<sup>32</sup> Based on these results, the multiple addition approach appears to be the most rational way to use the  $S_2O_5^{2-}$  reagent, and it was chosen hereafter to perform the degradation of the contaminants under study.

**2.2. Comparison of Metabisulfite ( $S_2O_5^{2-}$ ) and Hydrogen Peroxide in the Degradation of CECs.** The ability of Fe-TAML to activate metabisulfite was tested against the degradation of additional micropollutants. Figure 3 shows the

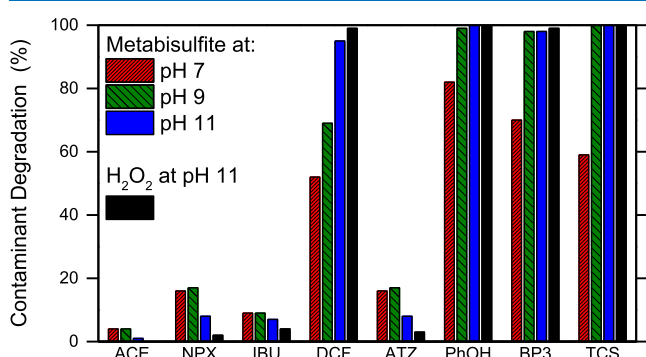


**Figure 3.** Degradation percentage of the studied CEC. Metabisulfite or  $H_2O_2$  were used as reagents at different pH values. The reactions were carried out for 60 min in phosphate buffer (10 mM), by adding 0.1 mM of the reagent every 10 min for a total of three additions (at 0, 10, and 20 min). Initial conditions were  $[Fe-TAML] = 0.01$  mM and  $[contaminant] = 0.1$  mM.

percentage of contaminant degradation after 1 h reaction time, when metabisulfite was used as the reagent at different pH values (7, 9, and 11). The reaction was carried out by adding 0.1 mM of metabisulfite for a total of three times, once every 10 min (i.e., with a final concentration of 0.3 mM). After the last addition, the system was monitored for an additional 40 min to observe possible further degradation of the tested contaminant (see Figures S2–S8 in the Supporting Information for the whole time trends). The same contaminants were also degraded following the analogous protocol but by using  $H_2O_2$  at pH 11 instead of  $S_2O_5^{2-}$ . This operational pH value was chosen because it is well known to maximize the degradation efficiency with the couple Fe-TAML/ $H_2O_2$ . The generally accepted reason for this pH behavior is twofold: (i) the Fe-TAML complex is involved in an acid–base equilibrium between the axial diaqua species  $[FeL(OH_2)_2]^-$  and the deprotonated form  $[FeL(OH_2)(OH)]^{2-}$  ( $L = TAML$ ,  $pK_a > 11$ ); at the same time, (ii)  $H_2O_2$  behaves as well like a weak acid with  $pK_a \approx 11.2$ – $11.6$ ;<sup>12</sup> see more details in the Supporting Information. Our experimental results suggest that metabisulfite and hydrogen peroxide have similar activity toward the chosen contaminants. Specifically, Fe-TAML could activate efficiently both  $S_2O_5^{2-}$  and  $H_2O_2$  in the degradation of the phenolic compounds BP3, TCS, and PhOH. Moreover, both processes were also efficient in the degradation of DCF. On the other hand, although metabisulfite was marginally more active than hydrogen peroxide toward acesulfame K (ACE), naproxen (NPX), ibuprofen (IBU), and atrazine (ATZ), both reagents were largely ineffective toward these contaminants. Replicate tests suggested high reproducibility of these reaction processes, with final degradation yields from different tests always within 5% of the average value; see Figure S9 in the

Supporting Information to see results from some test replicates.

Previous literature has reported that Fe-TAML forms an iron-oxo active species with peroxides.<sup>10,12,38</sup> The iron-oxo species is electrophilic, and it tends to react with electron-rich compounds that are easily oxidized. Coming back to our data, the complete degradation of PhOH and the inactivity of the process toward ACE (see Figure 3) are consistent with a peculiar role of oxidants with middle-high redox potential (such as iron-oxo species, *vide infra*) in both the Fe-TAML/ $H_2O_2$  and the Fe-TAML/ $S_2O_5^{2-}$  chemistry. Indeed, PhOH<sup>39</sup> is definitely electron richer than ACE<sup>40</sup> (see also the electrochemical evidences reported below). The results, in terms of the Fe-TAML +  $H_2O_2$  reaction efficiency, may thus be rationalized with the different electronic structure of the contaminants, in agreement with Chen and White.<sup>41</sup> Then, because metabisulfite showed the same efficiency trend as  $H_2O_2$  toward the chosen contaminants, we can tentatively assume as a working hypothesis that there is a close analogy between the reactive species involved in the two cases.

Interestingly, when the Fe-TAML +  $S_2O_5^{2-}$  process led to quantitative or almost quantitative substrate transformation (i.e., with PhOH, BP3, and TCS), the degradation efficiency was very similar at both pH 9 and 11, while the degradation at pH 7 was less effective. Conversely, when the degradation was inefficient (i.e., with ACE, NPX, IBU, and ATZ), it was so at all of the tested pH values. DCF is the only instance in which we observed a gradual increase of the degradation efficiency throughout the entire interval of increasing pH. Differently from DCF, the phenolic compounds PhOH, BP3, and TCS undergo acid–base equilibria in the pH interval 7–11, thereby yielding the corresponding easily oxidized phenolates at high pH.<sup>35</sup> For this reason, the case of DCF, which does not undergo acid–base equilibrium changes between pH 7 and 11, is likely to better reflect the genuine pH trend of the Fe-TAML +  $S_2O_5^{2-}$  reactivity. Note that a low Fe-TAML activity at pH 7 has already been reported in a previous paper describing the Fe-TAML activation of  $H_2O_2$ .<sup>12</sup>

Different from the classic Fenton reaction at acidic pH, which is mainly driven by the production of hydroxyl radicals<sup>42</sup> and is usually poorly selective toward different pollutants, the Fe-TAML-activated process was definitely more selective (see Figure 3). On the one hand, this means that a smaller number of contaminants can be targeted with Fe-TAML-Fenton compared to  $Fe^{2+} + H_2O_2$ . However, higher selectivity (i.e., the ability of the catalyst to discriminate amongst different compounds) might improve the degradation efficiency of target contaminants in a multipolluted aqueous environment, especially in the presence of interfering agents, such as the inherently harmless organic matter. Organic matter usually does not require a dedicated degradation step, but it is accidentally degraded by hydroxyl radicals and, by consuming them, it may inhibit the traditional Fenton process.<sup>43</sup> In contrast, by virtue of higher selectivity, iron-oxo-based treatments may be less prone to interferences from organic matter.

**2.3. Discussion on the Nature of the Active Species and the Reaction Mechanism.** While it is accepted that systems containing Fe-TAML +  $H_2O_2$  have an iron-oxo species as reactive transient,<sup>10,12,38</sup> there is no piece of information concerning the behavior of Fe-TAML +  $S_2O_5^{2-}$ , or the nature of the resulting active species. Indeed, this system is here described for the first time. As mentioned above, Fe-TAML +



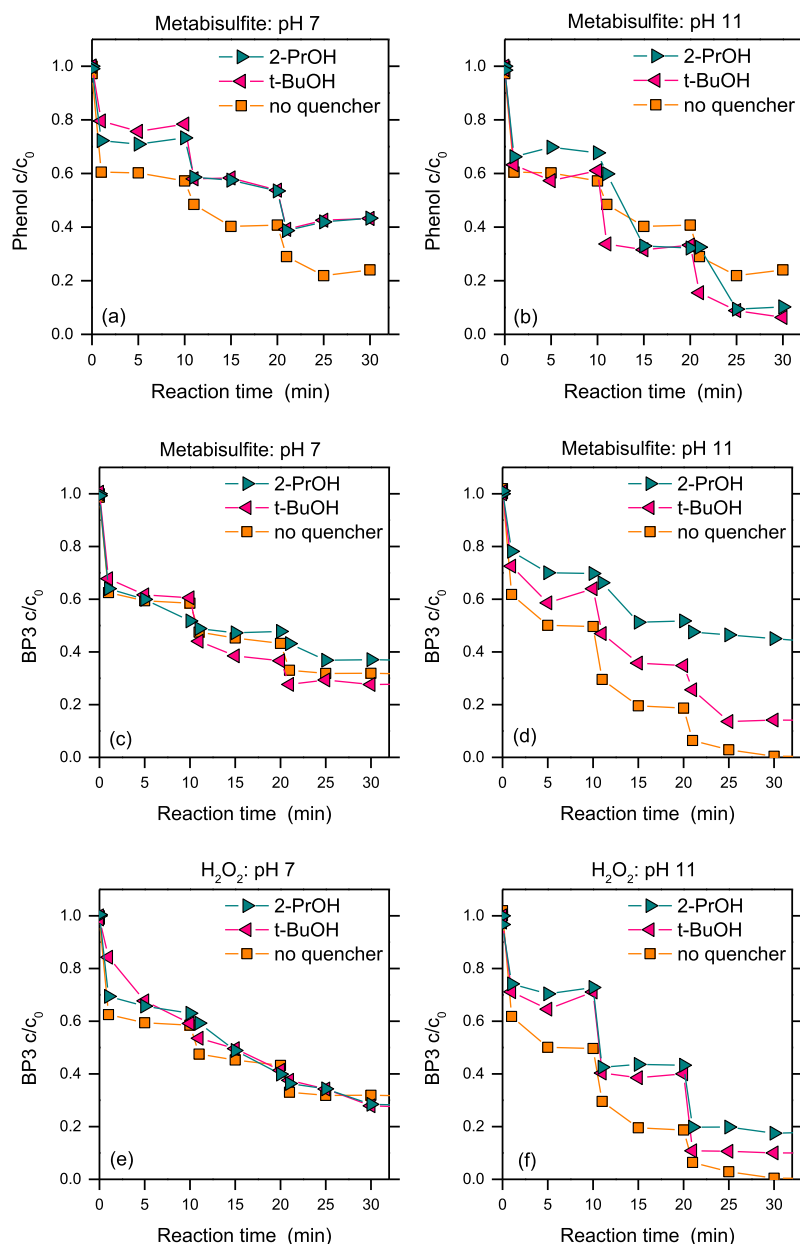


**Figure 4.** Effects of different quenchers on the degradation reaction. Quenchers were *t*-BuOH (40 mM) or 2-PrOH (133 mM), tested in the degradation of (a,b) phenol or (c–f) BP3. The reagents were (a–d) metabisulfite or (e,f)  $H_2O_2$ , and the pH was 7 (left column) or 11 (right column). Reactions were carried out in phosphate buffer (10 mM), adding 0.1 mM metabisulfite (or  $H_2O_2$ ) every 10 min, for a total of three additions (at 0, 10, and 20 min). Initial conditions were as follows:  $[Fe-TAML] = 0.01$  mM;  $[PhOH] = [BP3] = 0.1$  mM.

$H_2O_2$  and  $Fe-TAML + S_2O_5^{2-}$  had analogous reactivity at pH 11 toward the studied substrates. Therefore, it is reasonable to hypothesize that the formed active species share some similarities. Tests were conducted to assess whether the main active species of  $Fe-TAML + S_2O_5^{2-}$  has radical or nonradical nature. Although we could not rely on any previous report concerning the  $S_2O_5^{2-}$ -based Fenton process, possible reactive radical species in, for example, sulfite-based Fenton systems are hydroxyl ( $\bullet OH$ ) and sulfate ( $SO_4^{\bullet -}$ ).<sup>44</sup> In contrast, a Fe-based oxidant could trigger a nonradical pathway, in analogy with  $Fe-TAML + H_2O_2$ .

To get mechanistic insight into the studied process, *tert*-butanol (*t*-BuOH) and isopropyl alcohol (2-PrOH) were added into the solution as radical scavengers during the transformation of phenol. 2-PrOH is very reactive with

hydroxyl radicals ( $k = 1.9 \times 10^9$   $M^{-1} s^{-1}$ )<sup>13</sup> and significantly less so with sulfate radicals ( $k = 4 \times 10^7$   $M^{-1} s^{-1}$ ).<sup>45</sup> On the other hand, *t*-BuOH shows similar reactivity with both  $\bullet OH$  ( $k = 4 \times 10^8$   $M^{-1} s^{-1}$ ) and  $SO_4^{\bullet -}$  ( $k = 3.6 \times 10^8$   $M^{-1} s^{-1}$ ).<sup>13,45</sup> Different phenol degradation experiments were thus carried out with  $Fe-TAML$  and metabisulfite, in the presence of *t*-BuOH and 2-PrOH. Scavenger/phenol concentration ratios of 400:1 (*t*-BuOH) and 1330:1 (2-PrOH) were used. Considering the reaction rate constants of phenol/phenolate with  $\bullet OH$  ( $k_{PhOH}$  and  $k_{PhO^-} \approx 10^{10}$   $M^{-1} s^{-1}$ )<sup>13</sup> and  $SO_4^{\bullet -}$  ( $k_{PhOH} = 2.2 \times 10^9$   $M^{-1} s^{-1}$ ,<sup>46</sup>  $k_{PhO^-}$  unknown but possibly similar, and  $<10^{10}$   $M^{-1} s^{-1}$ ),<sup>13</sup> it is expected that *t*-BuOH causes a  $\sim 95\%$  inhibition of phenol degradation if  $\bullet OH$  is the reactive species (i.e., the degradation should be  $\sim 20$  times lower with the alcohol). Moreover, almost total quenching by *t*-BuOH is

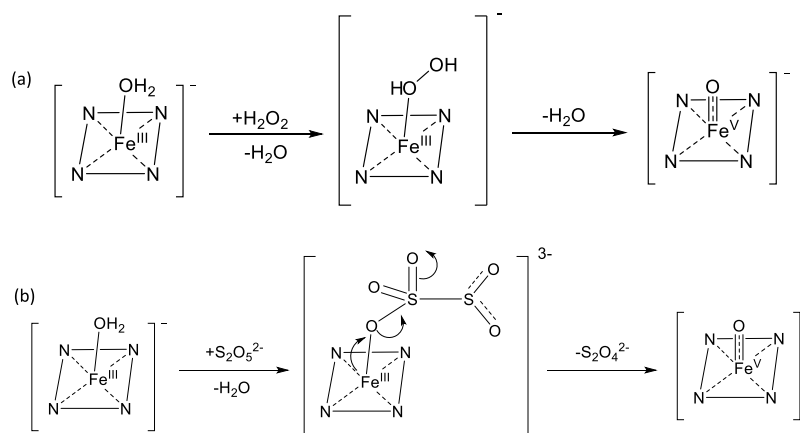


**Figure 5.** Reaction pathways in the activation of reagents by Fe-TAML. (a) Established pathway for the activation of hydrogen peroxide as discussed by Ghosh et al.,<sup>12</sup> and (b) proposed pathway for the activation of metabisulfite.

**Table 1.** Onset Potential for the Oxidation of the Studied Contaminants of Emerging Concern<sup>a</sup>

compound	oxidation onset (V vs Ag/AgCl) (V)	oxidation onset (1st scan, V vs Ag/AgCl) (V)	comments
ACE	0.90	0.90	Although an anodic current onset can be appreciated for ACE, the oxidation current is always very low and an anodic peak is never observed. In fact, for the analytical determination of ACE, Pierini et al. <sup>48</sup> have exploited its reduction. Because of limited solubility in $\text{CH}_3\text{CN}$ , the same measurement was repeated in water at pH 10. No anodic current was observed compared with the blank run
NPX	0.80	0.25	An additional oxidation peak could be appreciated on the first scan only. The potential of the anodic peak observed in the successive scans corresponds with literature data <sup>49</sup>
IBU	1.62	1.62	The oxidation onset potential corresponds very well to the results of Lima et al., <sup>50</sup> obtained using a boron-doped diamond
DCF	0.05	0.05	The results obtained are coherent with the literature. <sup>50</sup> Nevertheless, in that report, the authors reported significantly larger sensitivity in the 0 V/0.6 V potential window thanks to the modification of the glassy carbon electrode
ATZ	1.75	1.75	ATZ is only oxidized at a very positive potential. In fact, for ATZ determination, Svorc et al. <sup>51</sup> exploited its reduction
PhOH	0.70	0.80	The oxidation onset potential decreases on successive scans because of the formation of catechol and hydroquinone <sup>52</sup>
BP3	0.90	1.25	The anodic peak at 1.05 V (with corresponding oxidation onset at 0.9 V) is only observed if the potential is previously swept below 0 V. The main oxidation onset corresponds very well to the results reported by Sunyer et al. <sup>53</sup>
TCS	0.60	0.60	Very similar values have been found by Fotouhi et al. <sup>54</sup>

<sup>a</sup>The onset potential is reported for both the first and the successive scans of the CVs.

expected in the case of  $\text{SO}_4^{\bullet-}$ . Similarly, inhibition by ProH should be quantitative with  $\bullet\text{OH}$ , and in the order of  $\sim 90\%$  with  $\text{SO}_4^{\bullet-}$ .

The results shown in Figure 4a,b indicate that the alcohols caused limited inhibition of phenol degradation by Fe-TAML +  $\text{S}_2\text{O}_5^{2-}$  at pH 7 and practically no inhibition at pH 11. These results are not consistent with the occurrence of either  $\bullet\text{OH}$  or  $\text{SO}_4^{\bullet-}$  as the main reactive species, especially at the higher pH value (11), where we would expect inhibition to be much more evident in the case of a dominant role of the hydroxyl and sulfate radicals as reactive species of the process. Moreover, the two alcohols produced very similar and limited effects on the degradation of BP3, with both Fe-TAML +  $\text{H}_2\text{O}_2$  and Fe-TAML +  $\text{S}_2\text{O}_5^{2-}$ , at both pH 7 and 11 (see Figure 4c–f). This analogy in behavior further suggests that similar reactive species may be involved in Fe-TAML +  $\text{H}_2\text{O}_2$  and Fe-TAML +  $\text{S}_2\text{O}_5^{2-}$ . In the case of Fe-TAML +  $\text{H}_2\text{O}_2$ , the reactive species is well known to be of a nonradical nature.<sup>10,12,38</sup> By analogy, and given the overall results, it is reasonable to believe that an iron-oxo species may also occur in Fe-TAML +  $\text{S}_2\text{O}_5^{2-}$ . The limited, observed inhibition of the degradation process by alcohols would be due to the slight reactivity of the iron-oxo

species (less oxidant with respect to  $\bullet\text{OH}$  or  $\text{SO}_4^{\bullet-}$ , vide infra) toward ProH and *t*-BuOH, with no need to invoke radical-based reactions.

A tentative outline of the mechanism of activation of  $\text{H}_2\text{O}_2$  by Fe-TAML has already been proposed (Figure 5a).<sup>12</sup> It has been reported that the activation of  $\text{H}_2\text{O}_2$  occurs via the heterolytic cleavage of its O–O bond, after coordination to the iron center. The cleavage of the O–O bond is reasonably helped by proton transfer, followed by water release and formation of an iron-oxo complex.<sup>12</sup> Taking inspiration from the hydrogen peroxide activation mechanism, in the case of the Fe-TAML/metabisulfite system, it is reasonable to suggest that the initial formation of the Fe–O–SR intermediate may be followed by heterolytic O–S cleavage, yielding the related iron-oxo species (Figure 5b). This would also tentatively explain why persulfate was not activated by Fe-TAML (Figure 1c). In the case of unreactive persulfate, the coordination of iron(III) should involve either sulfonyl or peroxy oxygen. The former may be too stable for resonance, and the corresponding  $\pi^*$  orbital of the O–S fragment would be too distant from the reducing Fe(III) center, while the latter may be sterically hindered because of the geometry of the persulfate molecule.

Although this outline looks reasonable and agrees with the experimental data, further work is needed to confirm this rationalization and the related mechanisms.

The oxidation potentials recorded for the CECs studied in the present work by using the cyclic voltammetry (CV) technique (Table 1) are coherent with the mechanism here proposed. All of the CECs under study have oxidation onset potentials between 0.05 and 1.75 V versus Ag/AgCl. The reported values were obtained by averaging three CV scans (see Figures S10–S17 of the Supporting Information for the raw CV data).

These results are coherent with previously published values, although the experimental conditions are not fully comparable. The radicals  $\cdot\text{OH}$  or  $\text{SO}_4^{\cdot-}$  have more positive reduction potentials (2.5 V or above vs SHE, i.e., at least 2.2 V vs Ag/AgCl) in the pH window under investigation; thus, they are able to oxidize all of the CECs under study and lead to their degradation.<sup>47</sup> A less oxidant active species, such as the hypothesized iron-oxo one, could only effectively oxidize the most reducing CECs, while having negligible reactivity toward the least reducing substrates. In fact, the CECs here considered could be divided into two groups based on their redox potentials: ACE, ATZ, BP3, IBU, and NPX can only be oxidized at potentials larger than 0.8 V versus Ag/AgCl, while DCF, PhOH, and TCS can be oxidized at potentials lower than 0.8 V. The CECs of the first group are only marginally (<20%) abated by Fe-TAML/metabisulfite, with the notable exception of BP3. Indeed, BP3 degradation exceeded 80% at basic pH despite an onset potential as high as 0.90 V (1.25 V for the first scan, if the initial potential is more positive than 0.2 V). This implies that the redox behavior of BP3 and, consequently, its degradation with Fe-TAML/metabisulfite is hardly described by the onset potential only. In contrast, a first reduction step might trigger BP3 degradation. The compounds with oxidation potential below 0.8 V, that is, DCF, PhOH, and TCS were all significantly degraded by Fe-TAML +  $\text{S}_2\text{O}_5^{2-}$ , especially at pH 11, in agreement with the CV data. Hence, the hypothesized iron-oxo reactive intermediate should have a redox potential of around 0.8/1 V versus Ag/AgCl, which allows for the oxidation of compounds such as DCF, PhOH, and TCS, but it is insufficient to significantly degrade ACE, ATZ, IBU, and NPX.

Note that the CV profiles allow for a first qualitative description, but specific interactions between the active species and the substrate could activate additional mechanisms, which are not operational during the electrochemical oxidation processes at the glassy carbon electrode in  $\text{CH}_3\text{CN}$ . Conversely, kinetic limitations could impede some oxidation reactions, although they are thermodynamically possible.

### 3. EXPERIMENTAL SECTION

**3.1. Chemicals.** Fe(III)-TAML was purchased from GreenOx Catalysts Inc. (Pittsburgh, PA, U.S.A.). Sodium phosphate tribasic was obtained from Carlo Erba (Italy). All of the other reagents, buffer solutions, and solvents were purchased from Sigma-Aldrich. Water was of Milli-Q quality [total organic carbon (TOC) 2 ppb, resistivity  $\geq 18.2 \text{ M}\Omega \text{ cm}$ ].

**3.2. Preparation of the Fe-TAML Stock Solution.** A stock solution of Fe-TAML was prepared by dissolving 520 mg Fe-TAML in 200 mL of a sodium hydroxide solution (0.05 M). The supernatant of this solution was used for further experiments. UV–vis analysis was carried out to determine the effective Fe-TAML concentration at pH 7, by measuring light absorbance at 360 nm. From the known Fe-TAML absorption

coefficient ( $6600 \text{ M}^{-1} \text{ cm}^{-1}$ ), a stock solution with a concentration of 3.1 mM was prepared. The stability of the catalyst in solution was spectrophotometrically checked every month. The stock solution was stored refrigerated ( $4^\circ \text{C}$ ) under the  $\text{N}_2$  atmosphere.

**3.3. Protocol of the Oxidation Experiments.** Three different reagents (sodium sulfite,  $\text{SO}_3^{2-}$ , potassium metabisulfite,  $\text{S}_2\text{O}_5^{2-}$ , and sodium persulfate,  $\text{S}_2\text{O}_8^{2-}$ ) were preliminarily tested, and their reactivity was compared with that of hydrogen peroxide. The most reactive compound, namely, metabisulfite, was then chosen to carry out further degradation experiments on several contaminants. Finally, the reaction mechanism with metabisulfite was investigated. The degradation experiments were carried out at room temperature, under continuous stirring for a maximum of 60 min. Reactions were tested at different pH values (7, 9, and 11) in 10 mL of phosphate buffer (total concentration 0.01 M). Under such conditions, the demetallation of Fe-TAML via the general acid mechanism can be considered negligible.<sup>33,55</sup> As shown in previous literature reports, the demetallation kinetics of Fe-TAML increases as the pH decreases, or as the concentration of the buffering agents increases at constant pH. For these reasons, the phosphate buffer concentration used in this study was as low as reported in previous works.<sup>12,55</sup> It is important to note that the mechanism of demetallation has not yet been fully understood.

Unless otherwise stated, the default initial concentrations in the experiments were as follows: 0.01 mM of Fe-TAML, 0.1 mM of the target contaminant, and 0.1 mM of the reagent ( $\text{H}_2\text{O}_2$ ,  $\text{SO}_3^{2-}$ ,  $\text{S}_2\text{O}_5^{2-}$ , or  $\text{S}_2\text{O}_8^{2-}$ ). During some tests, stepwise additions of the reagent corresponding each to a 0.1 mM concentration in the reaction system were made every 10 min, for a total of three additions. In all of these latter cases, the overall molar ratio of the Fe-TAML/contaminant/reagent was 1:10:30. All of the reactions were quenched by decreasing the pH to a final value  $<3$ . Under acidic conditions, demetallation is promoted and the catalytic reaction is stopped as a consequence.<sup>33</sup> In some experiments involving metabisulfite, control tests were performed by analysis of the solutions immediately following reaction and without acidification. No significant differences in the concentration of contaminants were observed with or without acidification of the solution.

**3.4. Analytical Methods.** UV–vis spectrophotometric measurements were performed using a Cary 100 Scan double-beam instrument (Varian). The concentrations of contaminants in solution were monitored by HPLC coupled with diode array detection (HPLC-DAD). The adopted LaChrom Elite instrument (VWR-Hitachi) was equipped with a L-2200 Autosampler (injection volume 60  $\mu\text{L}$ ), a L-2130 quaternary pump for low-pressure gradients, a L-2300 column oven (set at  $40^\circ \text{C}$ ), and a L-2455 DAD detector. The column was a RP-C18 LiChroCART (VWR Int., length 125 mm, diameter 4 mm), packed with LiChrospher 100 RP-18 (5  $\mu\text{m}$  diameter).

The different test contaminants were always eluted in isocratic mode, with a mixture of A = 5.7 mmol  $\text{L}^{-1}$   $\text{H}_3\text{PO}_4$  in water and B = methanol, at a flow rate of 1  $\text{mL min}^{-1}$ . The following conditions were used ( $\lambda$  = detection wavelength,  $t_R$  = retention time): ACE (5% B,  $\lambda$  = 220 nm and  $t_R$  = 4 min); ATZ (60% B,  $\lambda$  = 221 nm and  $t_R$  = 4.5 min); diclofenac (DCF, 65% B,  $\lambda$  = 275 nm and  $t_R$  = 8 min); ibuprofen (IBU, 70% B,  $\lambda$  = 222 nm and  $t_R$  = 6 min); NPX (60% B,  $\lambda$  = 220 nm and  $t_R$  = 6 min); oxybenzone (aka benzophenone-3, BP3, 70% B,  $\lambda$  = 280 nm and  $t_R$  = 5 min); phenol (PhOH, 30% B,  $\lambda$  = 271 nm

and  $t_R = 5.5$  min); triclosan (TCS, 70% B,  $\lambda = 280$  nm and  $t_R = 9.6$  min).

Note that the study of the degradation of the investigated substrates cannot be considered in terms of the evolution of the TOC in solution, because (i) the Fe-TAML catalyst is in the homogeneous form and (ii) the organic TAML ligand increases the overall TOC value, thereby interfering with the assessment of contaminant mineralization. Still, the studied systems are unlikely to achieve substrate mineralization, as suggested by the occurrence of several unknown HPLC peaks, presumably accounted for by transformation intermediates (more hydrophilic than the original substrates on the basis of their chromatographic retention times), even at long reaction times.

**3.5. Electrochemical Measurements.** The redox properties and stability of the investigated substrates were electrochemically investigated. The electrochemical experiments were carried out through a standard photoelectrochemical setup and a computer-controlled potentiostat (PGSTAT12, Autolab). The electrochemical cell was a conventional three-electrode cell. The counter and reference electrodes were a glassy carbon rod (diameter 2 mm, length 75 mm) and a Ag/AgCl/KCl (3 M) electrode, respectively. The working electrode was a 5 mm diameter glassy carbon disk. The electrolytic solution was 0.1 M NaClO<sub>4</sub> in CH<sub>3</sub>CN, purged with nitrogen gas. CVs were recorded between  $-0.4$  and  $2.0$  V, at a scan rate of  $100$  mV s<sup>-1</sup>. To better detect the onset of the anodic current, CVs were recorded on 10 mM solutions of each studied compound, with the exceptions of ATZ and ACE. In the latter cases, CVs were recorded on saturated CH<sub>3</sub>CN solutions. The CVs here reported are the average of at least three successive scans, unless otherwise stated.

## ■ ASSOCIATED CONTENT

### ■ Supporting Information

The Supporting Information is available free of charge at <https://pubs.acs.org/doi/10.1021/acsomega.9b03088>.

Degradation percentages in all of the investigated conditions, together with the most significant experimental parameters; kinetic trends obtained from replicate experiments of the degradation of phenol, using metabisulfite as a reagent; details about the degradation efficiency of the Fe-TAML/hydrogen peroxide system as a function of pH; kinetic trends in the degradation of the different CECs; values of the degradation percentage of CEC from replicate experiments; and CV data from measurements performed with different CECs (PDF)

## ■ AUTHOR INFORMATION

### Corresponding Authors

\*E-mail: [davide.vione@unito.it](mailto:davide.vione@unito.it). Phone: +39 0116705296. Fax: +39 0116705242.

\*E-mail: [alberto.tirafferri@polito.it](mailto:alberto.tirafferri@polito.it). Phone: +39 0110907628. Fax: +39 0110907699.

### ORCID

Marco Minella: 0000-0003-0152-460X

Davide Vione: 0000-0002-2841-5721

Alberto Tirafferri: 0000-0001-9859-1328

### Notes

The authors declare no competing financial interest.

## ■ ACKNOWLEDGMENTS

D.V. acknowledges financial support by Università di Torino and Compagnia di San Paolo (project CSTO168282-ABATEPHARM). G.F. and A.T. acknowledge financial support by Politecnico di Torino.

## ■ ABBREVIATIONS

TAML, tetra-amido macrocyclic ligand; CEC, contaminants of emerging concern; ACE, acesulfame K; NPX, naproxen; IBU, ibuprofen; DCF, diclofenac; ATZ, atrazine; PhOH, phenol; TCS, triclosan; BP3, oxybenzone (benzophenone-3)

## ■ REFERENCES

- (1) Carvalho, R. N.; Ceriani, L.; Ippolito, A.; Lettieri, T. *Development of the First Watch List under the Environmental Quality Standards Directive*, 2015.
- (2) Pignatello, J. J.; Oliveros, E.; MacKay, A. Advanced oxidation processes for organic contaminant destruction based on the Fenton reaction and related chemistry. *Crit. Rev. Environ. Sci. Technol.* **2006**, *36*, 1–84.
- (3) Haber, F.; Weiss, J. Über die Katalyse des Hydroperoxydes. *Die Naturwissenschaften* **1932**, *20*, 948–950.
- (4) Koppenol, W. H. The Haber-Weiss cycle—70 years later. *Redox Rep.* **2001**, *6*, 229–234.
- (5) Duesterberg, C. K.; Mylon, S. E.; Waite, T. D. pH Effects on Iron-Catalyzed Oxidation using Fenton's Reagent. *Environ. Sci. Technol.* **2008**, *42*, 8522–8527.
- (6) Guengerich, F. P. Cytochrome P450 and chemical toxicology. *Chem. Res. Toxicol.* **2008**, *21*, 70–83.
- (7) Collins, T. J. TAML oxidant activators: A new approach to the activation of hydrogen peroxide for environmentally significant problems. *Accounts Chem. Res.* **2002**, *35*, 782–790.
- (8) Banerjee, D.; Markley, A. L.; Yano, T.; Ghosh, A.; Berget, P. B.; Minkley, E. G.; Khetan, S. K.; Collins, T. J. "Green" Oxidation Catalysis for Rapid Deactivation of Bacterial Spores. *Angew. Chem. Int. Ed.* **2006**, *45*, 3974–3977.
- (9) Beach, E. S.; Duran, J. L.; Horwitz, C. P.; Collins, T. J. Activation of Hydrogen Peroxide by an Fe-TAML Complex in Strongly Alkaline Aqueous Solution: Homogeneous Oxidation Catalysis with Industrial Significance. *Ind. Eng. Chem. Res.* **2009**, *48*, 7072–7076.
- (10) Chahbane, N.; Popescu, D.-L.; Mitchell, D. A.; Chanda, A.; Lenoir, D.; Ryabov, A. D.; Schramm, K.-W.; Collins, T. J. FeIII-TAML-catalyzed green oxidative degradation of the azodye Orange II by H<sub>2</sub>O<sub>2</sub> and organic peroxides: products, toxicity, kinetics, and mechanisms. *Green Chem.* **2007**, *9*, 49–57.
- (11) Mondal, S.; Hangun-Balkir, Y.; Alexandrova, L.; Link, D.; Howard, B.; Zandhuis, P.; Cugini, A.; Horwitz, C. P.; Collins, T. J. Oxidation of sulfur components in diesel fuel using Fe-TAML catalysts and hydrogen peroxide. *Catal. Today* **2006**, *116*, S54–S61.
- (12) Ghosh, A.; Mitchell, D. A.; Chanda, A.; Ryabov, A. D.; Popescu, D. L.; Upham, E. C.; Collins, G. J.; Collins, T. J. Catalase–Peroxidase Activity of Iron(III)–TAML Activators of Hydrogen Peroxide. *J. Am. Chem. Soc.* **2008**, *130*, 15116–15126.
- (13) Buxton, G. V.; Greenstock, C. L.; Helman, W. P.; Ross, A. B. Critical Review of rate constants for reactions of hydrated electrons, hydrogen atoms and hydroxyl radicals OH/•O– in Aqueous Solution. *J. Phys. Chem. Ref. Data* **1988**, *17*, 513–886.
- (14) Zhang, Y.; Zhou, M. A critical review of the application of chelating agents to enable Fenton and Fenton-like reactions at high pH values. *J. Hazard. Mater.* **2019**, *362*, 436–450.
- (15) Tang, L. L.; DeNardo, M. A.; Schuler, C. J.; Mills, M. R.; Gayathri, C.; Gil, R. R.; Kanda, R.; Collins, T. J. Homogeneous Catalysis Under Ultradilute Conditions: TAML/NaClO Oxidation of Persistent Metaldehyde. *J. Am. Chem. Soc.* **2017**, *139*, 879–887.
- (16) Canosa, P.; Rodríguez, I.; Rubi, E.; Rubi, N.; Cela, R. Formation of halogenated by-products of parabens in chlorinated water. *Anal. Chim. Acta* **2006**, *575*, 106–113.



- (17) Chowdhury, S.; Champagne, P.; McLellan, P. J. Models for predicting disinfection byproduct (DBP) formation in drinking waters: a chronological review. *Sci. Total Environ.* **2009**, *407*, 4189–4206.
- (18) Komulainen, H. Experimental cancer studies of chlorinated by-products. *Toxicology* **2004**, *198*, 239–248.
- (19) Allard, S.; Tan, J.; Joll, C. A.; von Gunten, U. Mechanistic Study on the Formation of Cl-/Br-/I-Trihalomethanes during Chlorination/Chloramination Combined with a Theoretical Cytotoxicity Evaluation. *Environ. Sci. Technol.* **2015**, *49*, 11105–11114.
- (20) Chekli, L.; Phuntsho, S.; Kim, J. E.; Kim, J.; Choi, J. Y.; Choi, J.-S.; Kim, S.; Kim, J. H.; Hong, S.; Sohn, J.; Shon, H. K. A comprehensive review of hybrid forward osmosis systems: Performance, applications and future prospects. *J. Membr. Sci.* **2016**, *497*, 430–449.
- (21) Li, D.; Yan, Y.; Wang, H. Recent advances in polymer and polymer composite membranes for reverse and forward osmosis processes. *Prog. Polym. Sci.* **2016**, *61*, 104–155.
- (22) Schreck, A.; Knorr, A.; Wehrstedt, K. D.; Wandrey, P. A.; Gmeinwieser, T.; Steinbach, J. Investigation of the explosive hazard of mixtures containing hydrogen peroxide and different alcohols. *J. Hazard. Mater.* **2004**, *108*, 1–7.
- (23) *Hydrogen Peroxide in Tooth Whitening Products*; European Commission, 2005.
- (24) Balahura, R. J.; Sorokin, A.; Bernadou, J.; Meunier, B. Origin of the Oxygen Atom in C–H Bond Oxidations Catalyzed by a Water-Soluble Metalloporphyrin. *Inorg. Chem.* **1997**, *36*, 3488–3492.
- (25) Brandt, C.; van Eldik, R. Transition Metal-Catalyzed Oxidation of Sulfur(IV) Oxides. Atmospheric-Relevant Processes and Mechanisms. *Chem. Rev.* **1995**, *95*, 119–190.
- (26) Wietzerbin, K.; Muller, J. G.; Jameton, R. A.; Pratviel, G.; Bernadou, J.; Meunier, B.; Burrows, C. J. Hydroxylation, Epoxidation, and DNA Cleavage Reactions Mediated by the Biomimetic Mn-TMPyP/O<sub>2</sub>/Sulfite Oxidation System†. *Inorg. Chem.* **1999**, *38*, 4123–4127.
- (27) Tanaka, T.; Fujii, M.; Mori, H.; Hirono, I. Carcinogenicity Test of Potassium Metabisulfite in Mice. *Ecotoxicol. Environ. Saf.* **1979**, *3*, 451–453.
- (28) Lavoie, J.-C.; Lachance, C.; Chessex, P. Antiperoxide Activity of Sodium Metabisulfite—a Double-Edged-Sword. *Biochem. Pharmacol.* **1994**, *47*, 871–876.
- (29) Shi, Y.; Zhan, X.; Ma, L.; Li, L.; Li, C. Evaluation of antioxidants using oxidation reaction rate constants. *Front. Chem. China* **2007**, *2*, 140–145.
- (30) Beach, E. S.; Malecky, R. T.; Gil, R. R.; Horwitz, C. P.; Collins, T. J. Fe-TAML/hydrogen peroxide degradation of concentrated solutions of the commercial azo dye tartrazine. *Catal. Sci. Technol.* **2011**, *1*, 437–443.
- (31) Gupta, S. S.; Stadler, M.; Noser, C. A.; Ghosh, A.; Steinhoff, B.; Lenoir, D.; Horwitz, C. P.; Schramm, K. W.; Collins, T. J. Rapid total destruction of chlorophenols by activated hydrogen peroxide. *Science* **2002**, *296*, 326–328.
- (32) Minella, M.; De Bellis, N.; Gallo, A.; Giagnorio, M.; Minero, C.; Bertinetti, S.; Sethi, R.; Tiraferri, A.; Vione, D. Coupling of Nanofiltration and Thermal Fenton Reaction for the Abatement of Carbamazepine in Wastewater. *ACS Omega* **2018**, *3*, 9407–9418.
- (33) Ghosh, A.; Ryabov, A. D.; Mayer, S. M.; Horner, D. C.; Prasuhn, D. E.; Sen Gupta, S.; Vuocolo, L.; Culver, C.; Hendrich, M. P.; Rickard, C. E. F.; Norman, R. E.; Horwitz, C. P.; Collins, T. J. Understanding the mechanism of H<sup>+</sup>-induced demetalation as a design strategy for robust iron(III) peroxide-activating catalysts. *J. Am. Chem. Soc.* **2003**, *125*, 12378–12379.
- (34) Minero, C.; Lucchiari, M.; Maurino, V.; Vione, D. A quantitative assessment of the production of OH and additional oxidants in the dark Fenton reaction: Fenton degradation of aromatic amines. *RSC Adv.* **2013**, *3*, 26443–26450.
- (35) Martell, A. E.; Smith, R. M.; Motekaitis, R. J. Critically Selected Stability Constants of Metal Complexes Database. *Standard Reference Data Program*; National Institute of Standards and Technology, U.S.: Gaithersburg, MD, 2004; Vol. 46.
- (36) Brust, M.; Fink, J.; Bethell, D.; Schiffrin, D. J.; Kiely, C. Synthesis and reactions of functionalised gold nanoparticles. *J. Chem. Soc., Chem. Commun.* **1995**, 1655–1656.
- (37) Luo, M.; Zhang, X.-H.; Darensbourg, D. J. An Examination of the Steric and Electronic Effects in the Copolymerization of Carbonyl Sulfide and Styrene Oxide. *Macromolecules* **2015**, *48*, 6057–6062.
- (38) de Oliveira, F. T.; Chanda, A.; Banerjee, D.; Shan, X.; Mondal, S.; Que, L.; Bominaar, E. L.; Munck, E.; Collins, T. J. Chemical and Spectroscopic Evidence for an FeV-Oxo Complex. *Science* **2007**, *315*, 835–838.
- (39) Nishimoto, K.; Fujishiro, R. Electronic structure of phenol. *Bull. Chem. Soc. Jpn.* **1958**, *31*, 1036–1040.
- (40) Popova, A. D.; Velcheva, E. A.; Stamboliyska, B. A. DFT and experimental study on the IR spectra and structure of acesulfame sweetener. *J. Mol. Struct.* **2012**, *1009*, 23–29.
- (41) Chen, M. S.; White, M. C. A Predictably Selective Aliphatic C–H Oxidation Reaction for Complex Molecule Synthesis. *Science* **2007**, *318*, 783–787.
- (42) Ahmed, M. M.; Barbati, S.; Doumenq, P.; Chiron, S. Sulfate radical anion oxidation of diclofenac and sulfamethoxazole for water decontamination. *Chem. Eng. J.* **2012**, *197*, 440–447.
- (43) Avetta, P.; Pensato, A.; Minella, M.; Malandrino, M.; Maurino, V.; Minero, C.; Hanna, K.; Vione, D. Activation of Persulfate by Irradiated Magnetite: Implications for the Degradation of Phenol under Heterogeneous Photo-Fenton-Like Conditions. *Environ. Sci. Technol.* **2015**, *49*, 1043–1050.
- (44) Méndez-Díaz, J.; Sánchez-Polo, M.; Rivera-Utrilla, J.; Canonica, S.; von Gunten, U. Advanced oxidation of the surfactant SDBS by means of hydroxyl and sulphate radicals. *Chem. Eng. J.* **2010**, *163*, 300–306.
- (45) Neta, P.; Huie, R. E.; Ross, A. B. Rate Constants for Reactions of Inorganic Radicals in Aqueous Solution. *J. Phys. Chem. Ref. Data* **1988**, *17*, 1027–1284.
- (46) Boukari, S. O. B.; Pellizzari, F.; Karpel Vel Leitner, N. Influence of persulfate ions on the removal of phenol in aqueous solution using electron beam irradiation. *J. Hazard. Mater.* **2011**, *185*, 844–851.
- (47) Wardman, P. Reduction Potentials of One-Electron Couples Involving Free Radicals in Aqueous Solution. *J. Phys. Chem. Ref. Data* **1989**, *18*, 1637–1755.
- (48) Pierini, G. D.; Llamas, N. E.; Frago, W. D.; Lemos, S. G.; Di Nezio, M. S.; Centurión, M. E. Simultaneous determination of acesulfame-K and aspartame using linear sweep voltammetry and multivariate calibration. *Microchem. J.* **2013**, *106*, 347–350.
- (49) Suryanarayanan, V.; Zhang, Y.; Yoshihara, S.; Shirakashi, T. Voltammetric assay of naproxen in pharmaceutical formulations using boron-doped diamond electrode. *Electroanalysis* **2005**, *17*, 925–932.
- (50) Lima, A. B.; Torres, L. M. F. C.; Guimaraes, C. F. R. C.; Verly, R. M.; da Silva, L. M.; Carvalho, A. D.; dos Santos, W. T. P. Simultaneous Determination of Paracetamol and Ibuprofen in Pharmaceutical Samples by Differential Pulse Voltammetry Using a Boron-Doped Diamond Electrode. *J. Braz. Chem. Soc.* **2014**, *25*, 478–483.
- (51) Švorc, L.; Rievaj, M.; Bustin, D. Green electrochemical sensor for environmental monitoring of pesticides: Determination of atrazine in river waters using a boron-doped diamond electrode. *Sens. Actuators, B* **2013**, *181*, 294–300.
- (52) Safavi, A.; Maleki, N.; Tajabadi, F. Highly stable electrochemical oxidation of phenolic compounds at carbon ionic liquid-electrode. *Analyst* **2007**, *132*, 54–58.
- (53) Sunyer, A.; González-Navarro, A.; Serra-Roig, M. P.; Serrano, N.; Díaz-Cruz, M. S.; Díaz-Cruz, J. M. First application of carbon-based screen-printed electrodes for the voltammetric determination of the organic UV filters oxybenzone and octocrylene. *Talanta* **2019**, *196*, 381–388.
- (54) Fotouhi, L.; Shahbaazi, H. R.; Fatehi, A.; Heravi, M. M. Voltammetric Determination of Triclosan in Waste Water and Personal Care Products. *Int. J. Electrochem. Sci.* **2010**, *5*, 1390–1398.

(55) Polshin, V.; Popescu, D.-L.; Fischer, A.; Chanda, A.; Horner, D. C.; Beach, E. S.; Henry, J.; Qian, Y.-L.; Horwitz, C. P.; Lente, G.; Fabian, I.; Münck, E.; Bominaar, E. L.; Ryabov, A. D.; Collins, T. J. Attaining control by design over the hydrolytic stability of Fe-TAML oxidation catalysts. *J. Am. Chem. Soc.* **2008**, *130*, 4497–4506.